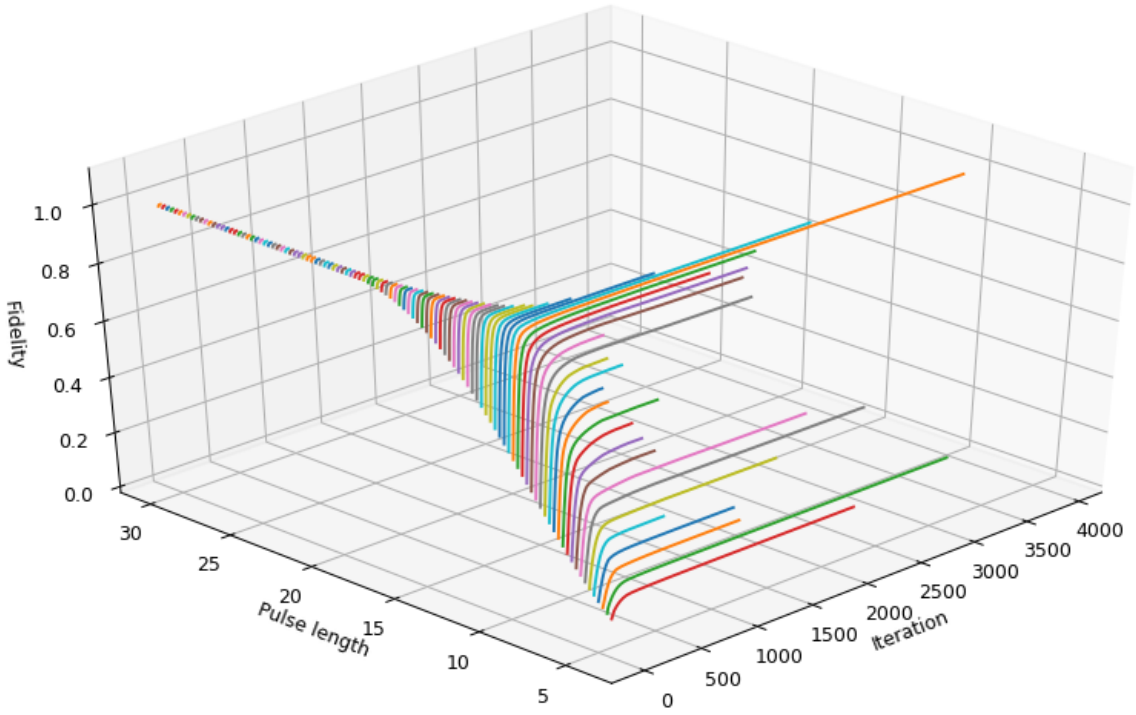


**Figure 1.1:** Fidelity during optimizations for every pulse length (ns). The different colors help distinguish the lines.

# 1 Results

The results of the numerical experiments will be presented in this chapter. For both optimization targets the optimized pulses, their properties and the final evolved state will be presented.

## 1.1 $|0\rangle \rightarrow |1\rangle$ state transfer

In fig. 1.1 the fidelity during all optimization runs are plotted. For pulse lengths longer than 15 ns the fidelity starts at values close to the goal ($F > 0.9$) and the number of iterations is relatively low (less than 85 iterations). In contrast, pulses shorter than 15 ns start at lower fidelities while the number of iterations are roughly one order of magnitude larger with no clear pattern.

To give a more detailed picture, the starting fidelity and optimized fidelity is plotted over pulse length in fig. 1.2. The optimizations where the fidelity goal was not reached, pulse lengths equal to and below 10.50 ns, are marked with stars.

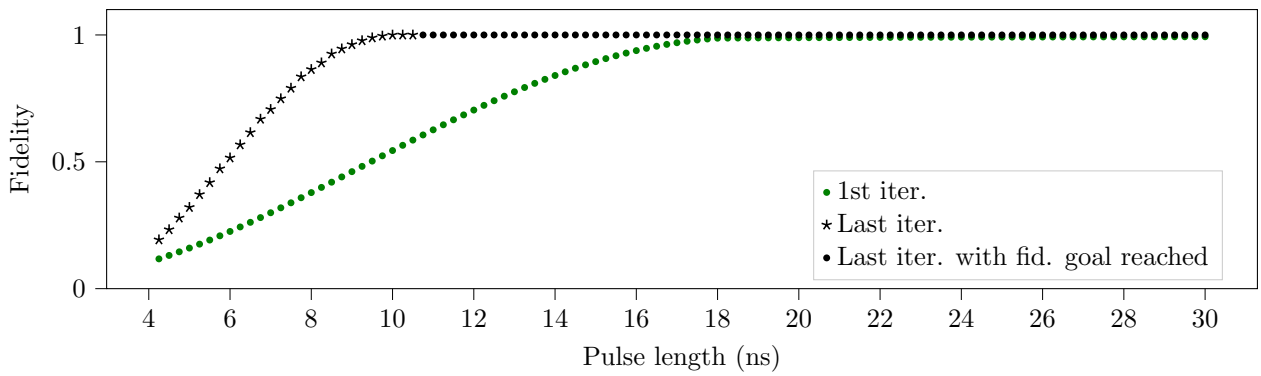


**Figure 1.2:** Fidelity of first and last iteration of every pulse length. The stable region above

Further analysis is done on pulses with lengths 4.25 ns, 6.0 ns, 8.0 ns, 10.0 ns, 20.0 ns and 30.0 ns. The optimized pulse shapes Re($\Omega$) and Im($\Omega$) are plotted in fig. 1.3 together with the guess pulses. Pulses longer than 20 ns require only fine adjustments to the Blackman guess pulse while shorter pulses have an imaginary part which is maximized for the whole duration of the pulse.

The spectrum of $\Omega(t)$ in the lab frame ($\Omega(t)e^{i\omega_{01}t}$) is shown in fig. 1.4. For all pulse lengths there is a peak centered roughly at $\omega_{01}$ and the width of the peak becomes narrower for longer pulses. For the highest pulse length 30 ns there is almost no support at $\omega_{02}$ and $\omega_{12}$.

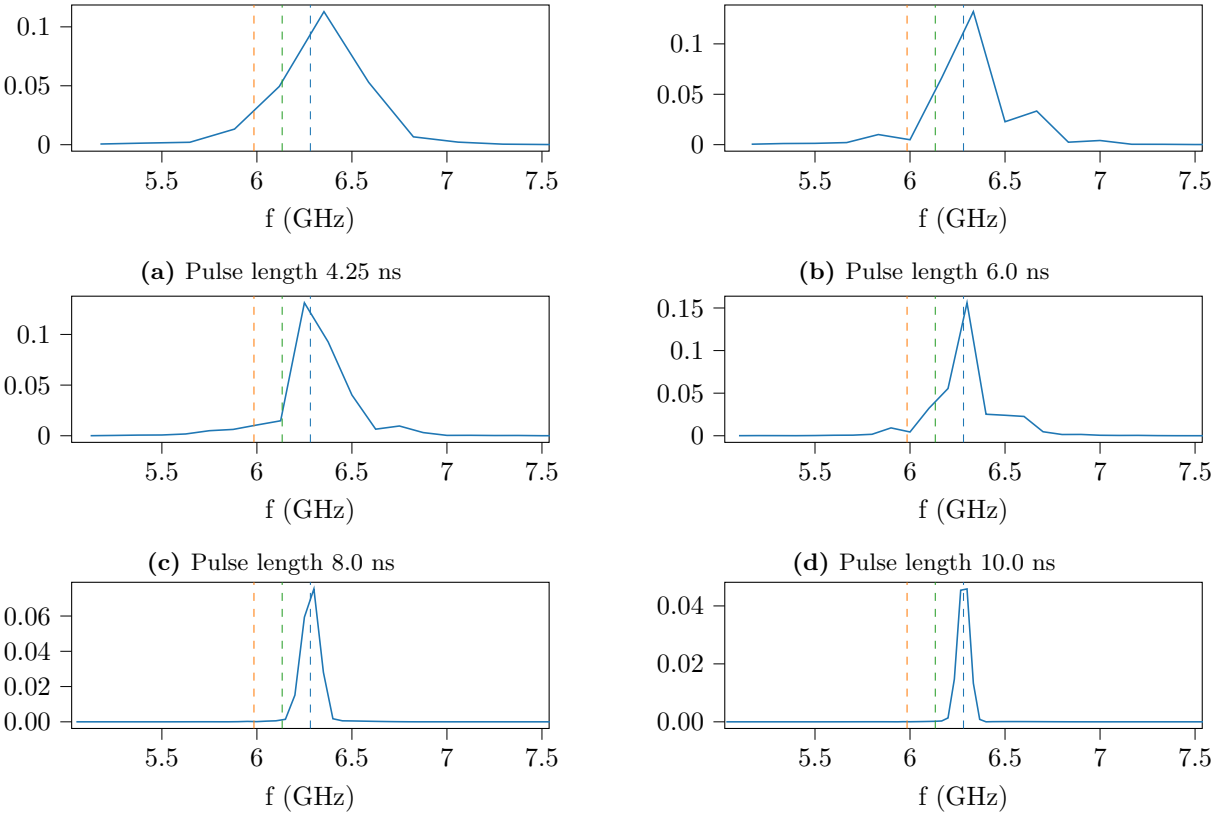


**(a)** Pulse length 4.25 ns

**(b)** Pulse length 6.0 ns

**(c)** Pulse length 8.0 ns

**(d)** Pulse length 10.0 ns

**(e)** Pulse length 20.0 ns

**(f)** Pulse length 30.0 ns

**Figure 1.4:** Pulse spectrum of the complex pulses in fig. 1.3. The vertical lines indicate (from left to right) $\omega_{02}$, $\omega_{12}$, $\omega_{01}$.

The time evolution of the system under the optimized pulses are visualized by plotting the occupation of the states over time, fig. 1.5, the projection of the state on the Bloch sphere over time, fig. 1.6, and a Hinton diagram of the evolved final state, fig. 1.7.

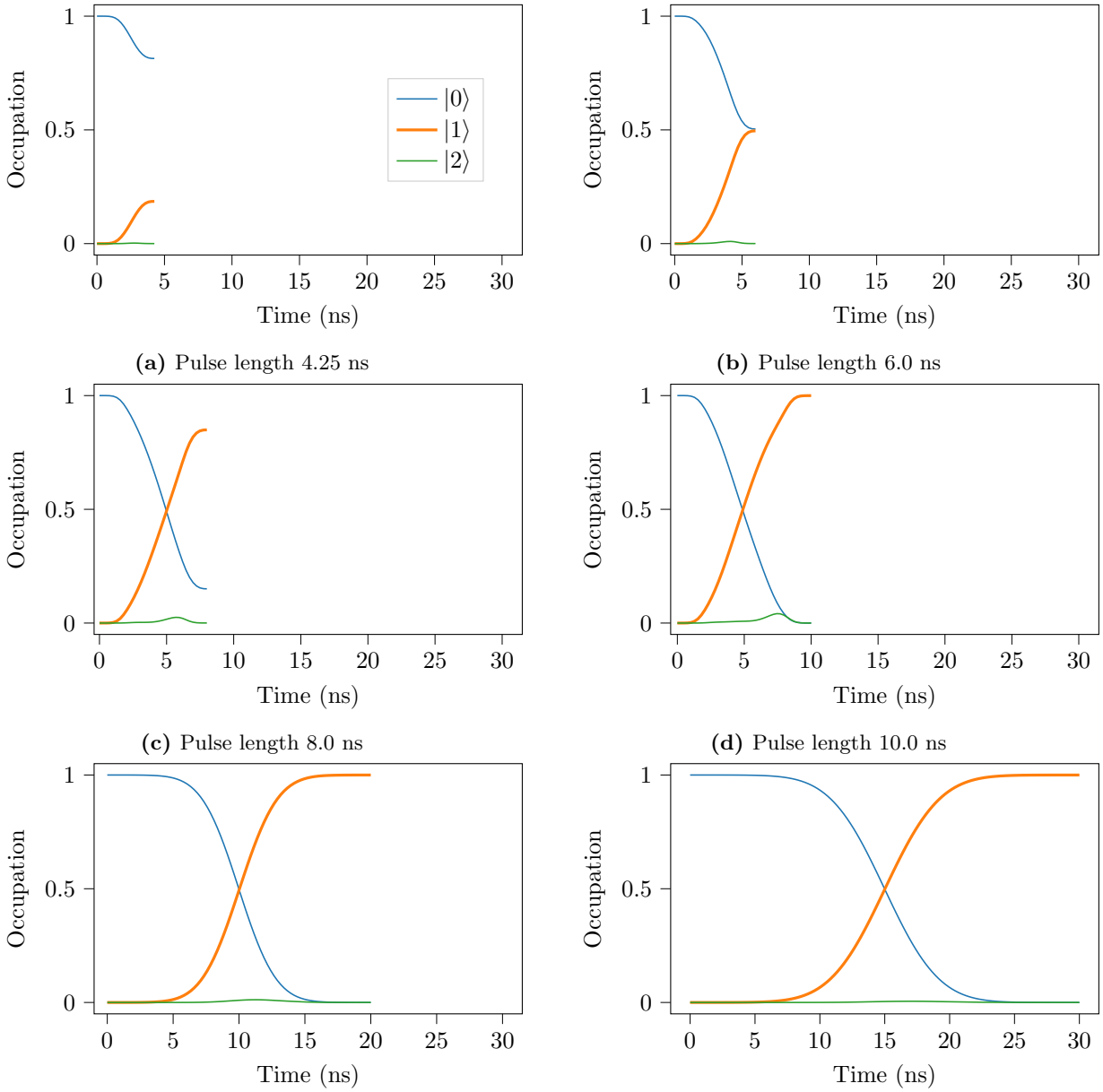


**(a)** Pulse length 4.25 ns

**(b)** Pulse length 6.0 ns

**(c)** Pulse length 8.0 ns

**(d)** Pulse length 10.0 ns

**(e)** Pulse length 20.0 ns

**(f)** Pulse length 30.0 ns

**Figure 1.5:** Energy level occupation over time for different lengths of optimized pulses.

For short pulse lengths there is not enough time for the transfer from $|0\rangle$ to $|1\rangle$, but for a pulse length of roughly 10.0 ns the goal is reached. Figure 1.5 **(b)** shows a little rise in occupation of $|2\rangle$ around 7.5 ns.

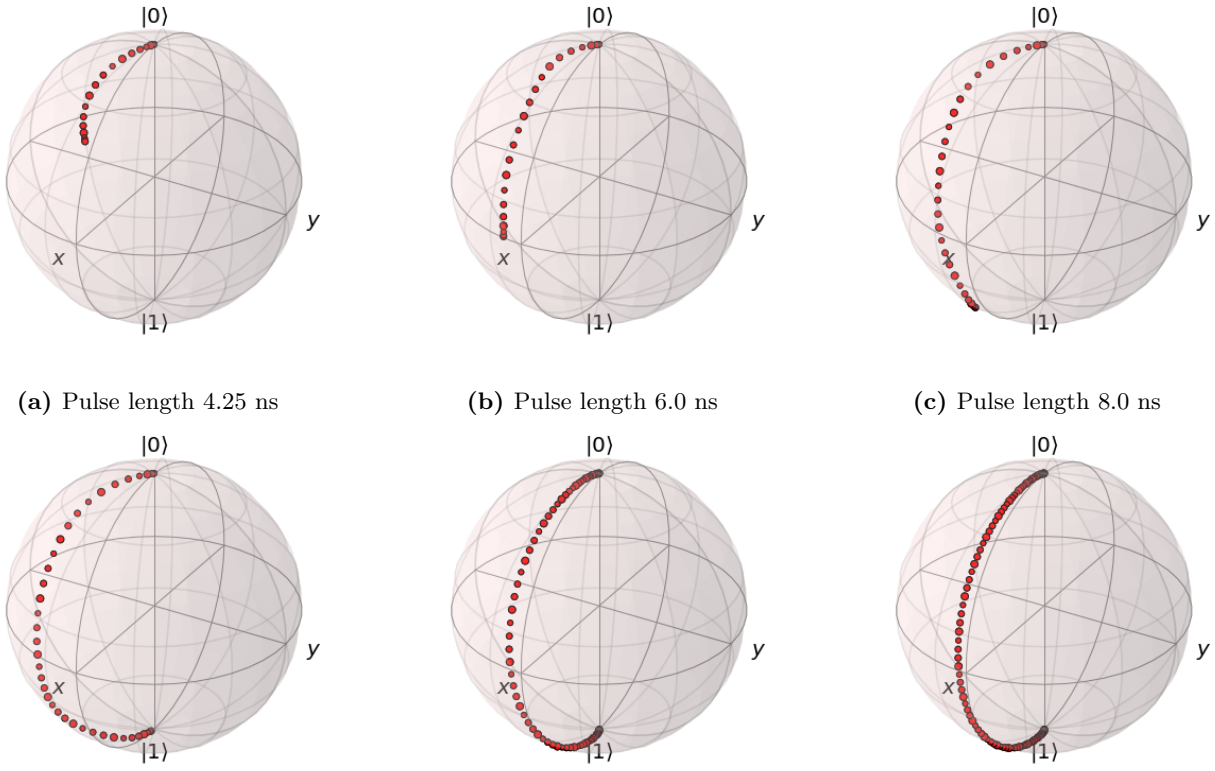


**(a)** Pulse length 4.25 ns **(b)** Pulse length 6.0 ns **(c)** Pulse length 8.0 ns

**(d)** Pulse length 10.0 ns **(e)** Pulse length 20.0 ns **(f)** Pulse length 30.0 ns

**Figure 1.6:** Time dynamics on the Bloch sphere for different lengths of optimized pulses.

Looking at fig. 1.6 we see that the transfer occurs along the y-axis for longer pulses.

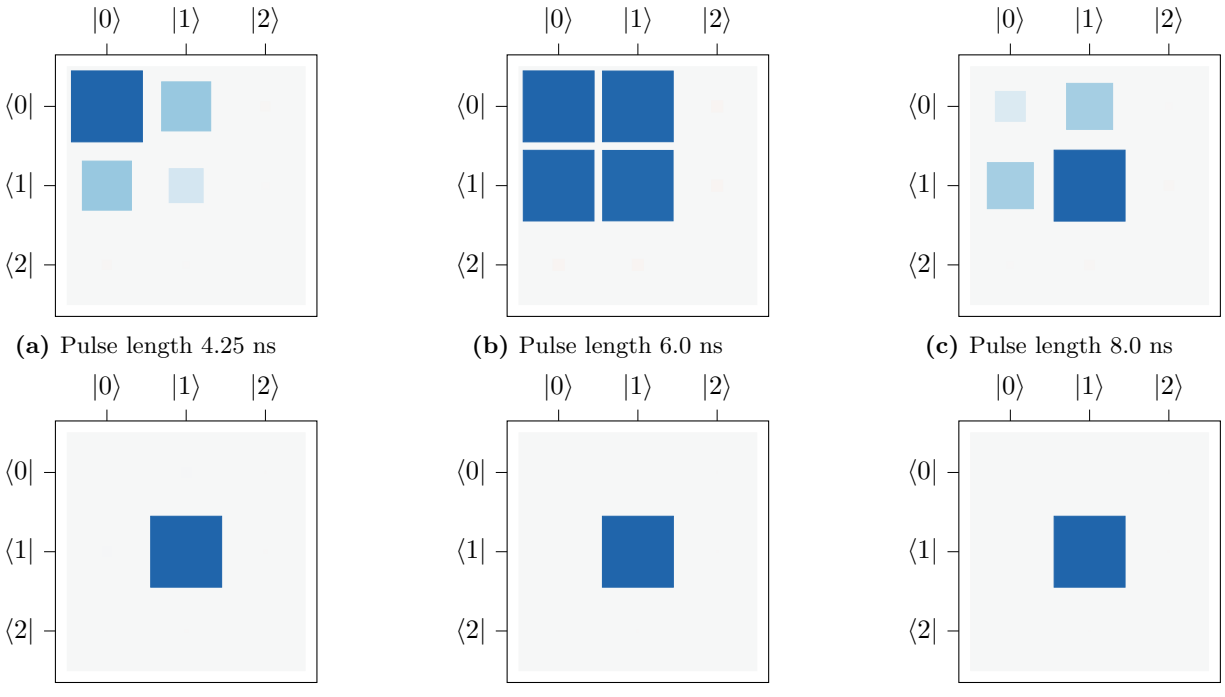


**(a)** Pulse length 4.25 ns **(b)** Pulse length 6.0 ns **(c)** Pulse length 8.0 ns

**(d)** Pulse length 10.0 ns **(e)** Pulse length 20.0 ns **(f)** Pulse length 30.0 ns

**Figure 1.7:** Hinton diagram of $|\psi(T)\rangle\langle\psi(T)|$

The Hinton diagram in fig. 1.7 provides a visualization of the density matrix $|\psi(T)\rangle\langle\psi(T)|$. The final density matrix shows how the much of the state is in the

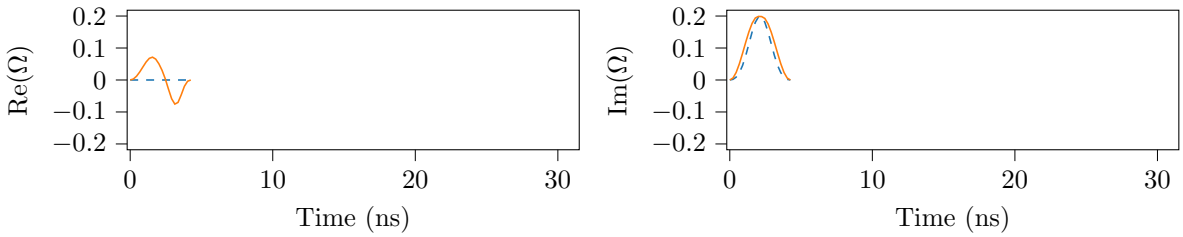


**(a)** Pulse length 4.25 ns

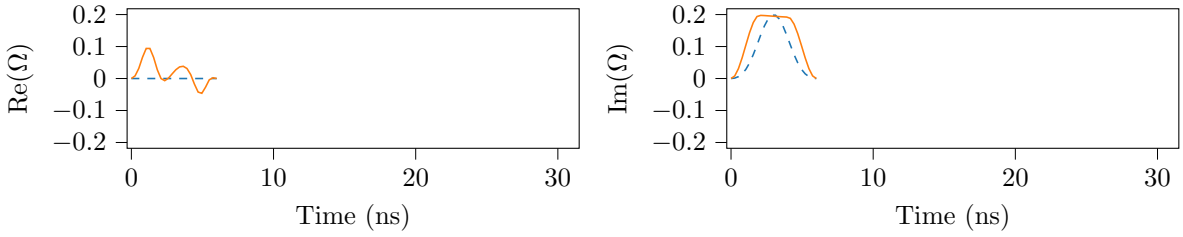


**(b)** Pulse length 6.0 ns

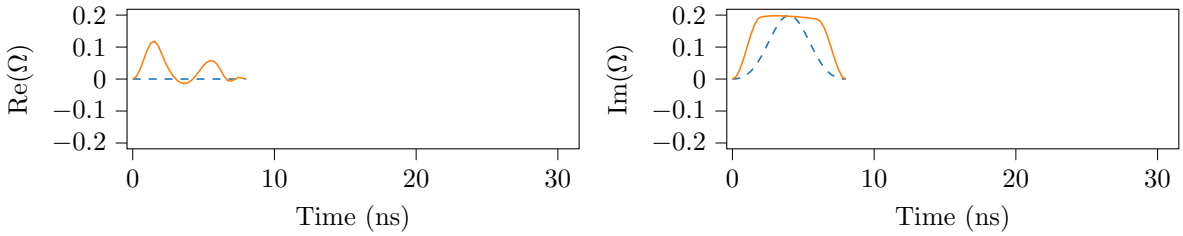


**(c)** Pulse length 8.0 ns

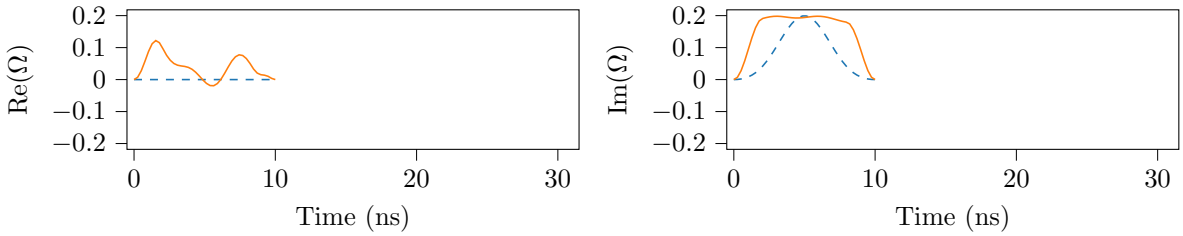


**(d)** Pulse length 10.0 ns

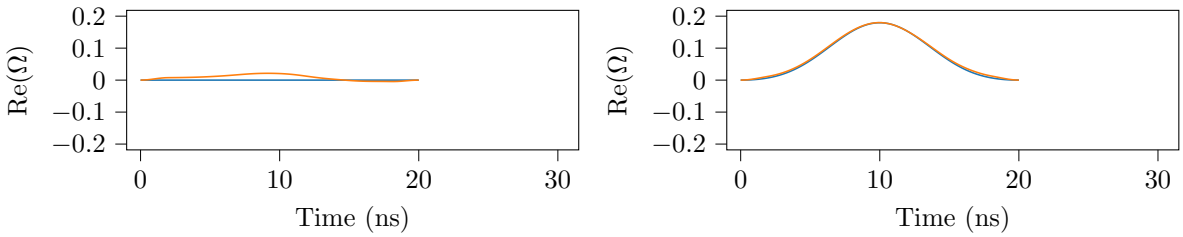


**(e)** Pulse length 20.0 ns

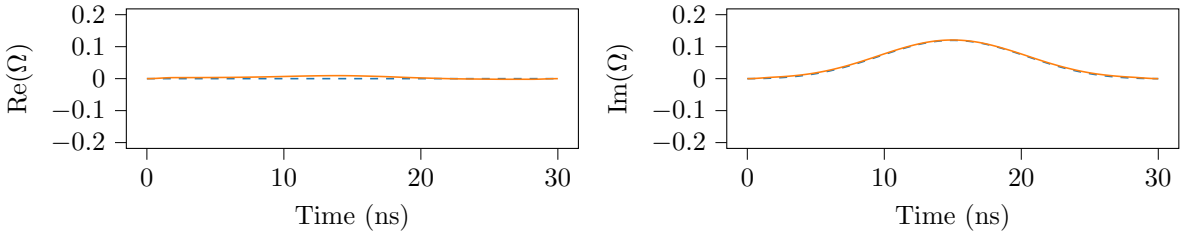


**(f)** Pulse length 30.0 ns

**Figure 1.3:** Optimised pulse shapes and guess pulses for pulse lengths **(a)** 4.25 ns, **(b)** 6.0 ns, **(c)** 8.0 ns, **(d)** 10.0 ns, **(e)** 20.0 ns, and **(f)** 30.0 ns. Short pulses (<10 ns) change substantially from the starting Blackman shape while long pulses (>20 ns) only require fine adjustments.

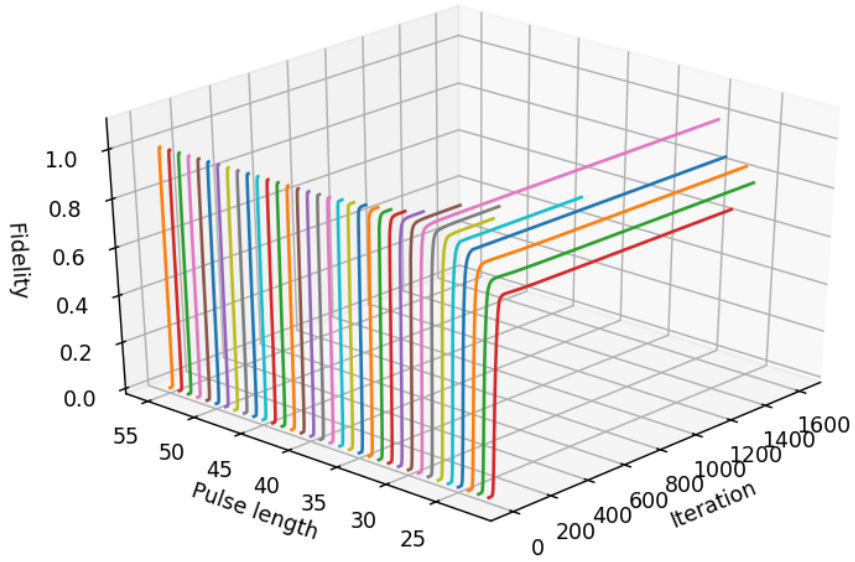


**Figure 1.8:** Fidelity during optimizations for every pulse length (ns).

## 1.2 $|0\rangle \rightarrow |2\rangle$ state transfer

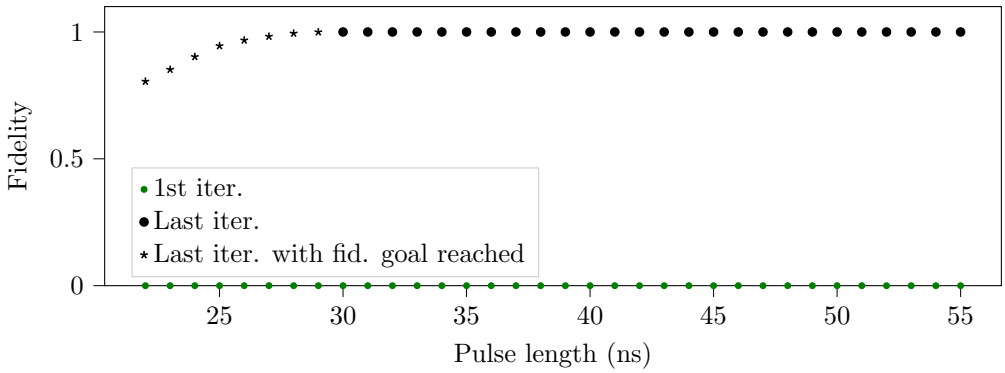


**Figure 1.9:** Fidelity of first and last iteration of every pulse length.

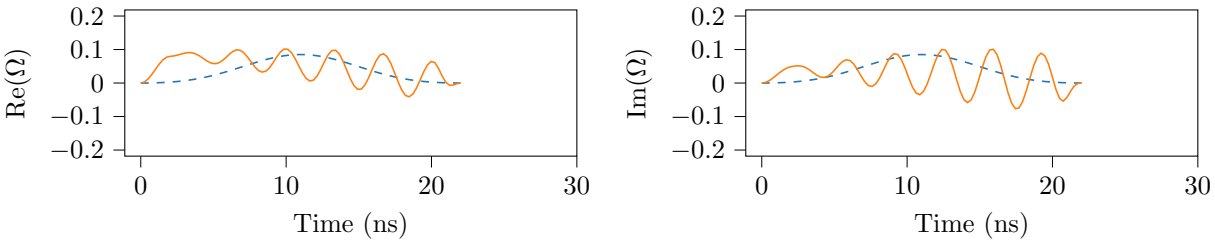


**(a)** Pulse length 22.0 ns

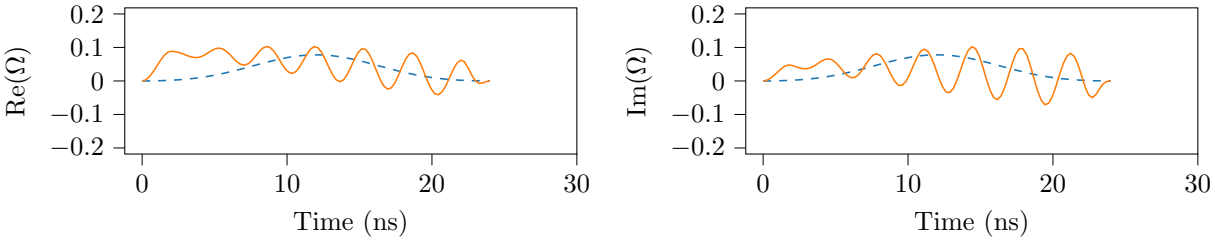


**(b)** Pulse length 24.0 ns

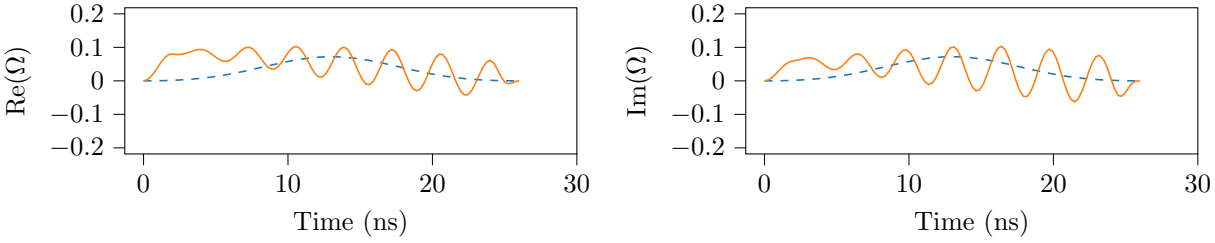


**(c)** Pulse length 26.0 ns

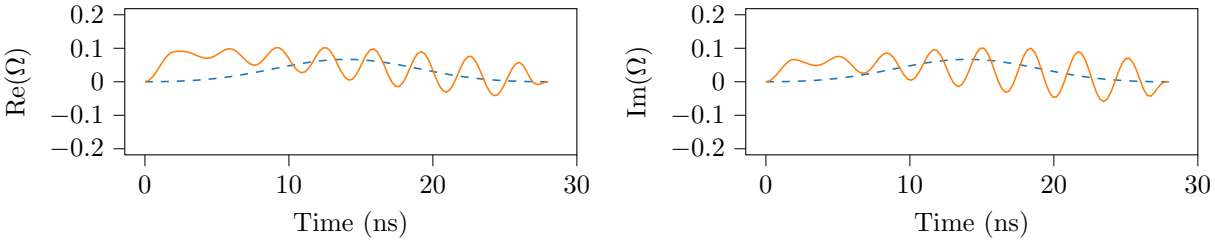


**(d)** Pulse length 28.0 ns

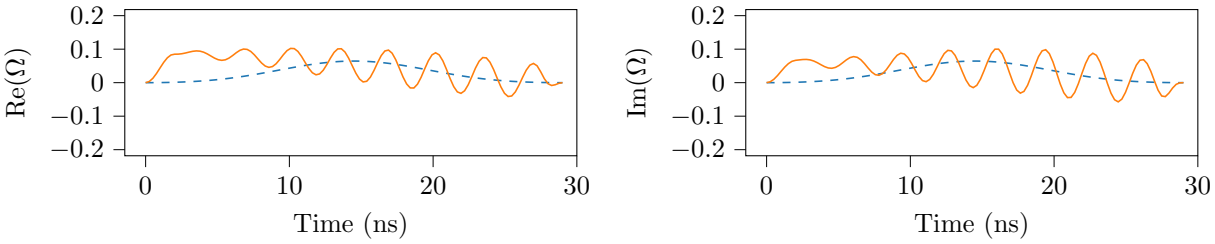


**(e)** Pulse length 29.0 ns

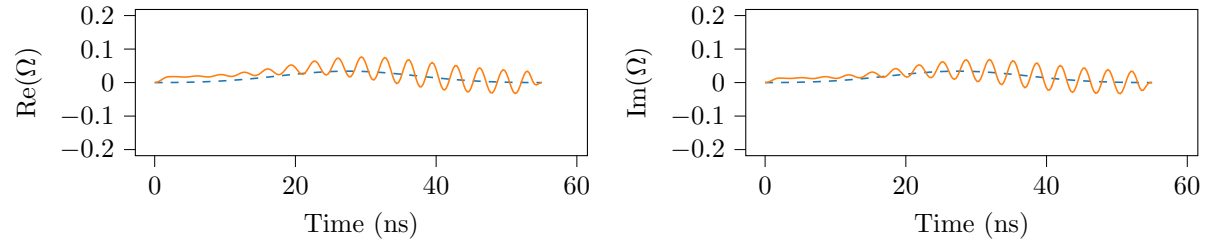


**(f)** Pulse length 55.0 ns

**Figure 1.10:** Pulse shapes.

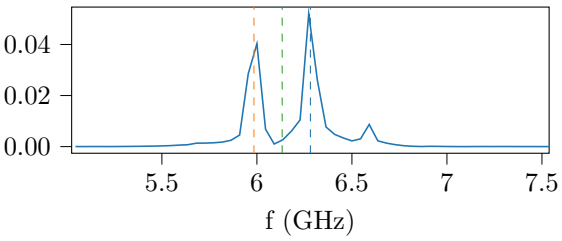


**(a)** Pulse length 22.0 ns

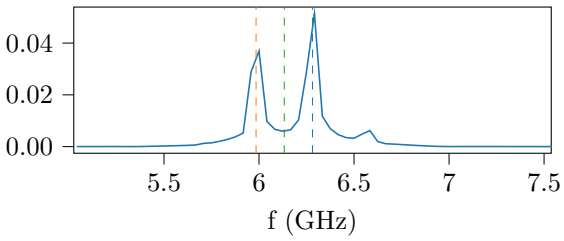


**(b)** Pulse length 24.0 ns

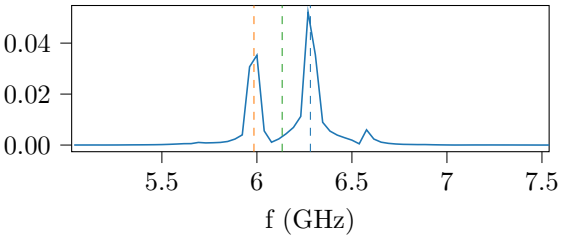


**(c)** Pulse length 26.0 ns

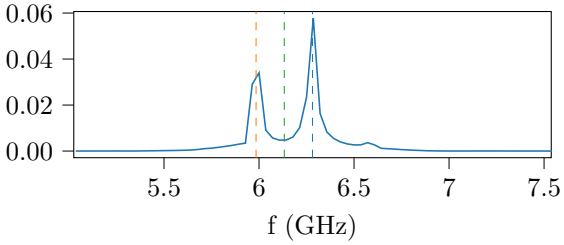


**(d)** Pulse length 28.0 ns

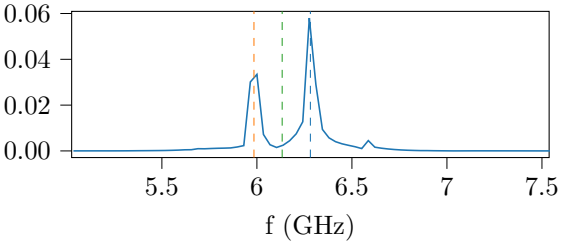


**(e)** Pulse length 29.0 ns

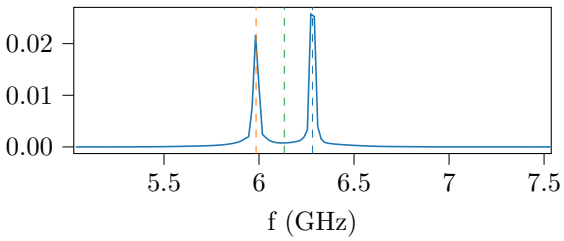


**(f)** Pulse length 55.0 ns

**Figure 1.11:** Pulse spectrum

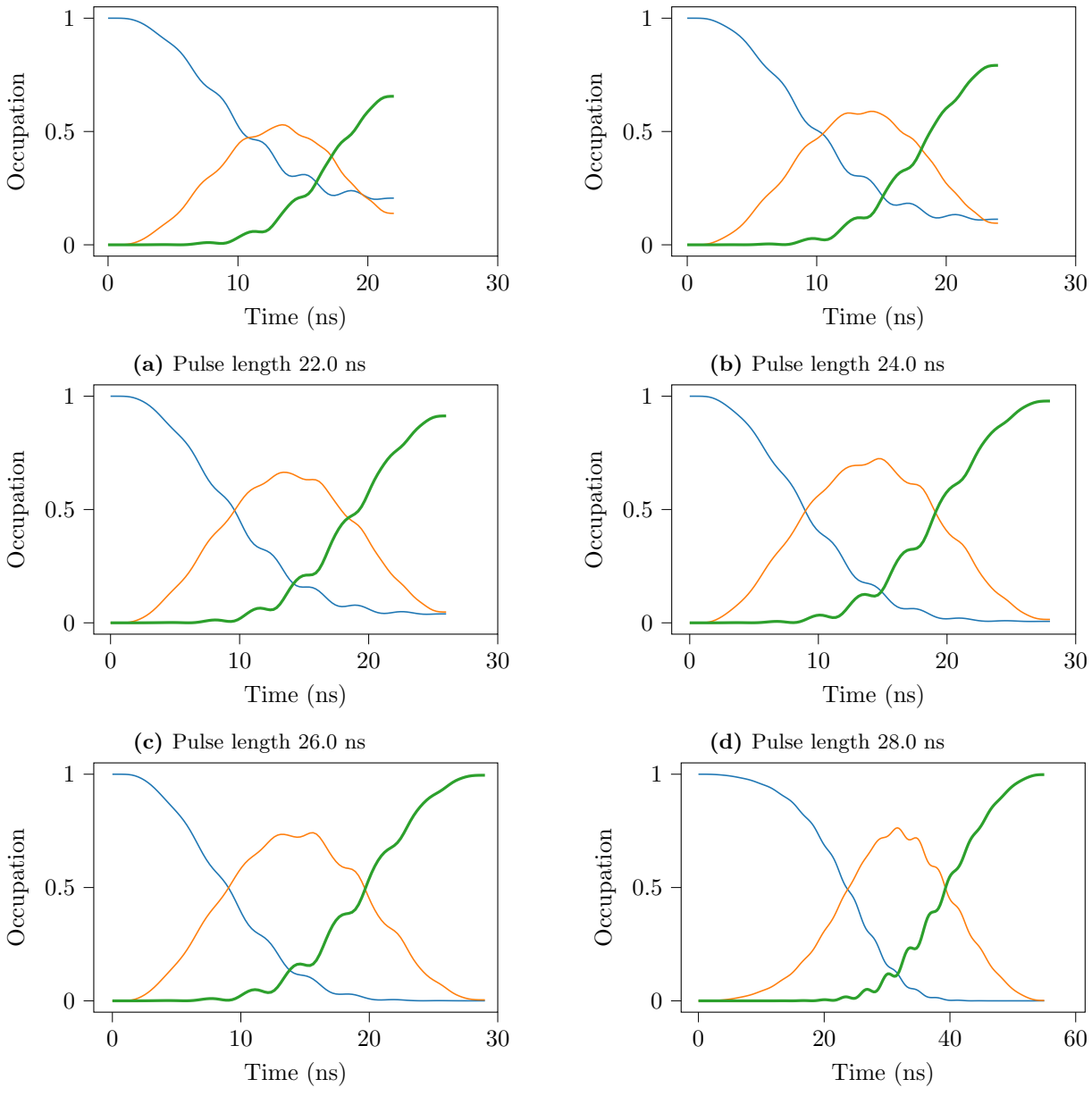


**(a)** Pulse length 22.0 ns

**(b)** Pulse length 24.0 ns

**(c)** Pulse length 26.0 ns

**(d)** Pulse length 28.0 ns

**(e)** Pulse length 29.0 ns

**(f)** Pulse length 55.0 ns

**Figure 1.12:** Energy level occupation over time for different lengths of optimized pulses.

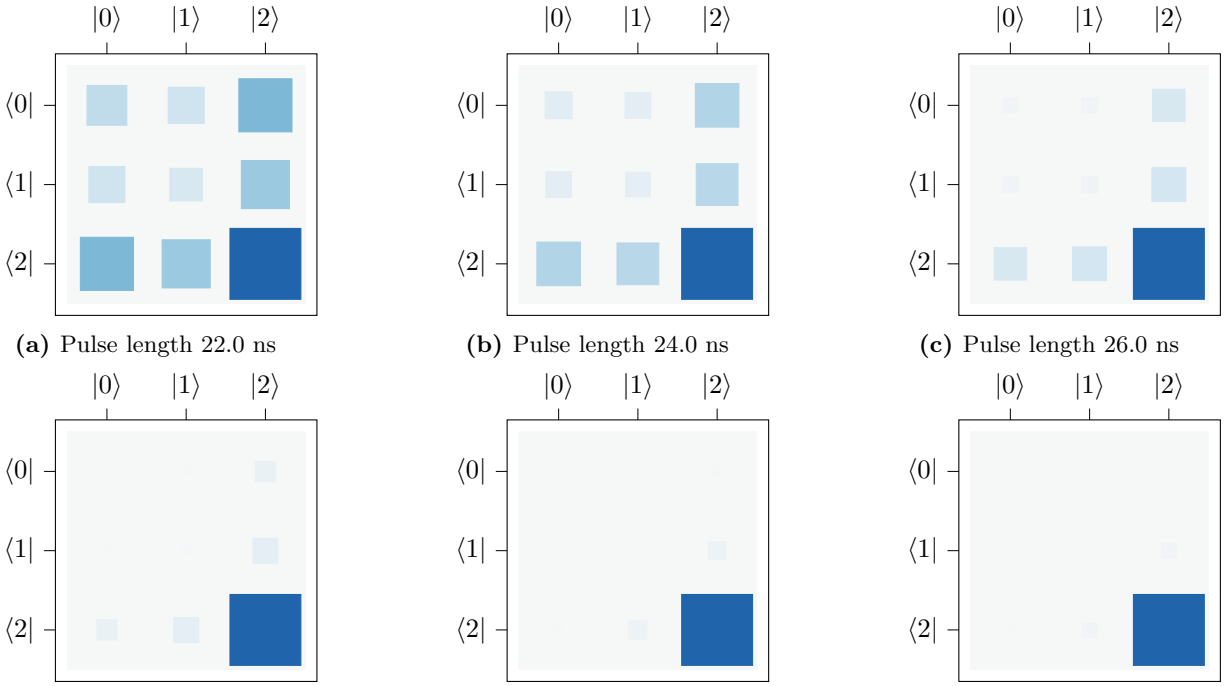


**(a)** Pulse length 22.0 ns **(b)** Pulse length 24.0 ns **(c)** Pulse length 26.0 ns

**(d)** Pulse length 28.0 ns **(e)** Pulse length 29.0 ns **(f)** Pulse length 55.0 ns

**Figure 1.13:** Hinton diagram of $|\psi(T)\rangle\langle\psi(T)|$

### 1.2.1 $|1\rangle_q |0\rangle_r \rightarrow |0\rangle_q |C_1\rangle_r$ state transfer

In this composite system it can be hard to see

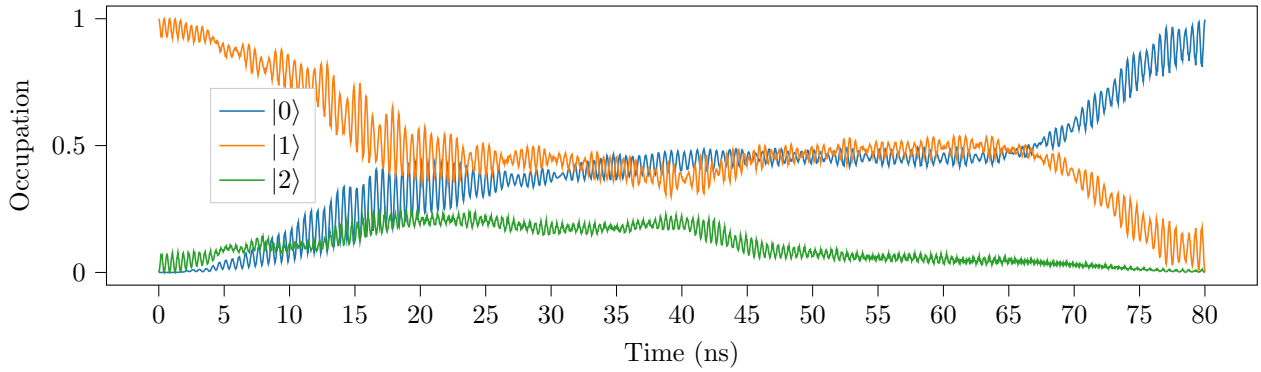


**Figure 1.14:** Occupation probability of the qubit over time.

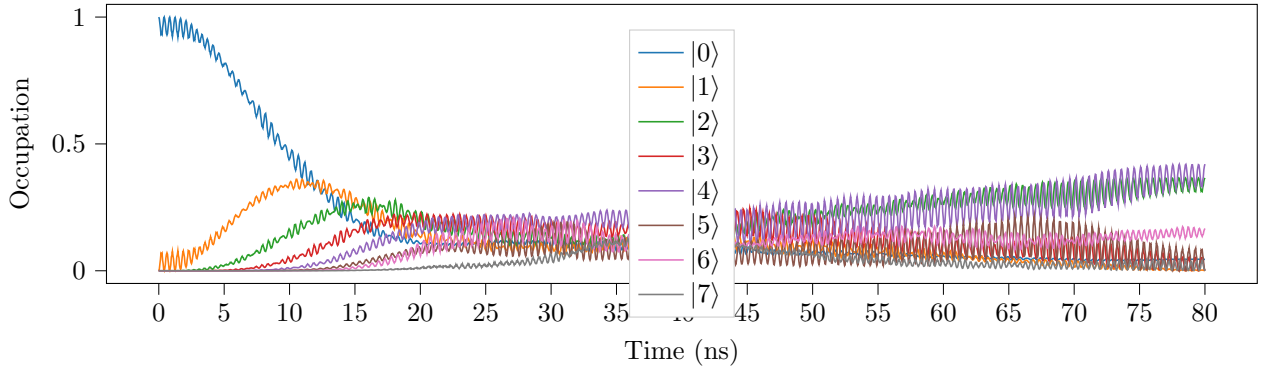


**Figure 1.15:** Occupation probability of the resonator over time.

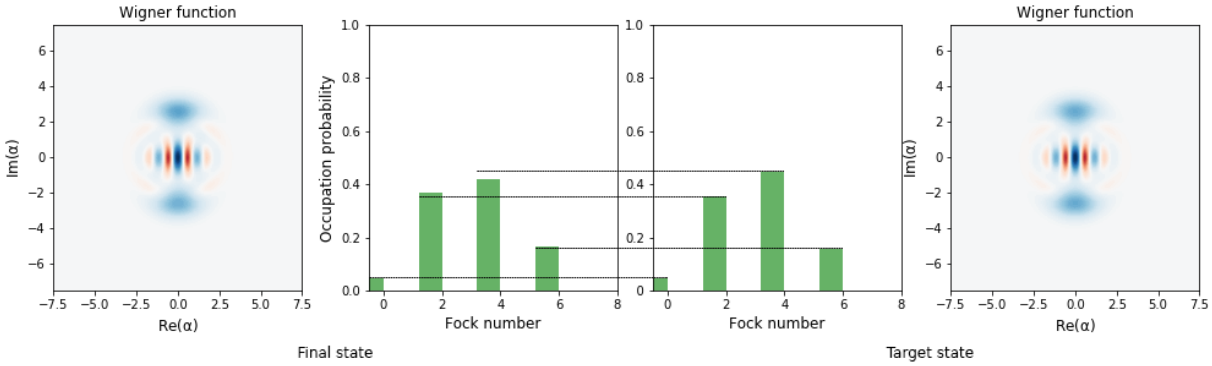


**Figure 1.16:** Comparison of the Fock distribution and Wigner function of $|\psi(T)\rangle$ and $|\psi_{\text{tar}}\rangle$.